Impact of nonlinear radiative nanoparticles on an unsteady flow of a Williamson fluid toward a permeable convectively heated shrinking sheet

Aurang Zaib
Department of Mathematical Sciences, Federal Urdu University of Arts Sciences and Technology, Karachi, Pakistan
Rizwan Ul Haq
Department of Electrical Engineering, Bahria University Islamabad, Islamabad, Pakistan
A.J. Chamkha
Mechanical Engineering Department, Prince Mohammad Bin Fahd University, Al-Khobar, Saudi Arabia and
RAK Research and Innovation Center, American University of Ras Al Khaimah, Ras al-Khaimah, United Arab Emirates, and
M.M. Rashidi
Department of Civil Engineering, School of Engineering, University of Birmingham, Birmingham, UK

Abstract

Purpose – The study aims to numerically examine the impact of nanoparticles on an unsteady flow of a Williamson fluid past a permeable convectively heated shrinking sheet.

Design/methodology/approach – In sort of the solution of the governing differential equations, suitable transformation variables are used to get the system of ODEs. The converted equations are then numerically solved via the shooting technique.

Findings – The impacts of such parameters on the velocity profile, temperature distribution and the concentration of nanoparticles are examined through graphs and tables. The results point out that multiple solutions are achieved for certain values of the suction parameter and for decelerating flow, while for accelerating flow, the solution is unique. Further, the non-Newtonian parameter reduces the fluid velocity and boosts the temperature distribution and concentration of nanoparticles in the first solution, while the reverse drift is noticed in the second solution.

Practical implications – The current results may be used in many applications such as biomedicine, industrial, electronics and solar energy.

Originality/value – The authors think that the current results are new and significant, which are used in many applications such as biomedicine, industrial, electronics and solar energy. The results have not been considered elsewhere.

Keywords Nanofluid, Unsteady flow, Convective boundary condition, Nonlinear radiation, Williamson fluid

Paper type Research paper

Nomenclature

a,c,d = positive constants;
A = unsteady parameter;
A_1 = first Rivilin–Erickson tensor;
$\ddot{C}$ = concentration of nanoparticles;
C_f = skin friction coefficient;
c_p = specific heat;
D_B = Brownian diffusion;
D_T = coefficients of thermophoresis diffusion;
f = dimensionless stream function;
h_f = coefficient of heat transfer;
I = identity tensor;
k = thermal conductivity;
$\ddot{k}^*$ = mean absorption coefficient;
$\ddot{m}_w$ = mass flux;
Nb = Brownian motion parameter;
Nt = thermophoresis parameter;
$Nu_{\breve{x}}$ = local Nusselt number;
Pr = Prandtl number;
q_r = radiative heat flux;
$\ddot{q}_w$ = heat flux;
$\mathrm{Re}_{\breve{x}}$ = local Reynolds number;
R_d = radiation parameter;
$\ddot{S}$ = Cauchy stress tensor;
S = suction parameter;
Sc = Schmidt number;
$\ddot{t}$ = time;

The current issue and full text archive of this journal is available on Emerald Insight at: **www.emeraldinsight.com/1708-5284.htm**

World Journal of Engineering
15/6 (2018) 731–742

[DOI 10.1108/WJE-02-2018-0050]

Received 12 February 2018
Revised 3 March 2018
16 March 2018
19 March 2018
Accepted 20 March 2018

$\ddot{T}$ = temperature;
$\ddot{T}_f$ = temperature of the hot fluid;
$\ddot{T}_\infty$ = free stream temperature;
$\ddot{T}_w$ = fluid wall temperature;
$\ddot{v}_w$ = variable velocity of suction;
v_0 = positive constant;
$\ddot{u}, \ddot{v}$ = velocity components; and
$\ddot{x}, \ddot{y}$ = Cartesian coordinates.

Greek symbols

$\ddot{\alpha}$ = thermal diffusivity;
δ = Williamson parameter;
$\ddot{\varepsilon}$ = extra stress tensor;
γ = convective parameter;
π = second invariant tensor;
θ = dimensionless temperature;
θ_w = temperature ratio parameter;
ν = kinematic viscosity;
$\ddot{\mu}_0$ = limiting viscosity at zero shear stress;
$\ddot{\mu}_\infty$ = limiting viscosity at infinite shear stress;
$(\rho cp)f$ = specific heat capacitance of nanofluid;
$\ddot{\tau}$ = ratio b/w the heat capacity and specific heat capacitance of nanoparticle;
$\ddot{\tau}_w$ = shear stress in x-direction;
$\ddot{\sigma}^*$ = Stefan–Boltzmann constant;
ψ = stream function;
η = similarity variable; and
$\ddot{\Gamma}$ = time constant.

Subscripts

w = condition at wall; and
∞ = condition at free stream.

Superscripts

$'$ = derivative w.r.t. η.

1. Introduction

There are several fluids of engineering and industrial significance such as multi-grade oils, blood polymers, petroleum production, composite material, fruit juices and shampoos that display the viscoelastic behavior. These fluids cannot be described by a simple model of Newtonian fluids. Owing to diversity of flow in nature, different non-Newtonian models have been recommended by researchers. Among several models, there is one important non-Newtonian model, which is the Williamson fluid model. The Williamson fluid model has a definite advantage over other non-Newtonian fluid models in that it contains both minimum and maximum viscosities, which give better results for pseudoplastic fluids (apparent viscosity at infinity does not tend to zero). Williamson (1927) proposed this model, which describes the equations of viscous flow of the pseudo-plastic fluids and verified the results experimentally. Nadeem *et al.* (2013) developed the two-dimensional flow equations of Williamson fluid toward a stretched surface and obtained the series solution using homotopy analysis method. Khan and Khan (2014) obtained the series solution of four types of steady flow of Williamson liquid. The two-dimensional steady flow of a Williamson fluid past a stretched sheet filled with nanoparticles was inspected by Nadeem and Hussain (2014). Malik and Salahuddin (2015) obtained the numerical result of MHD viscous flow of a Williamson fluid by stagnation point toward a stretched cylinder. Krishnamurthy *et al.* (2016) scrutinized the flow with MHD heat transfer of a Williamson liquid past a stretched sheet immersed in nanofluid with chemical reaction. The importance of the chemical reaction on three dimensional flow of a non-Newtonian Prandtl fluid over a Riga convectively heated surface was discussed by Kumar *et al.* (2017a). Recently, Kumar *et al.* (2017b) considered the effect of nonlinear thermal radiation on non-Newtonian Williamson fluid comprising dusty particles suspended on stretched surface. Very recently, Kumar *et al.* (2018) scrutinized the influences of magnetic and thermal radiation effects on flow of hyperbolic tangent dusty fluid past a stretched surface.

Nowadays, the investigation of nanofluids has received admirable interest owing to its various practical applications. Nanofluids are homogenous combination of nanoparticles and base or regular fluids similar to water, bio fluids, oil, ethylene glycol and other common liquids. As regular fluids have lower thermal conductivity, it is insufficient to assemble the necessity of today's rate of cooling. A dependable method to improve the thermal conductivity is to add in nanoparticles in regular fluid. Masuda *et al.* (1993) scattered the nanoparticles in fluid to enhance the thermal conductivity. Buongiorno (2006) observed that the thermophoresis diffusion and Brownian motion of nanoparticles give the immense enhancement in fluids thermal conductivity. Owing to these effects, he suggested the modifications in the convective situations. Nield and Kuznetsov (2009, 2010) initially considered the flow along a vertical sheet with nanofluid. Later on, Khan and Pop (2010) expanded Nield and Kuznetsov work by considering a constant surface temperature comprising nanofluid over a stretched surface. The characteristics of heat transfer comprising nanoparticles toward a convectively heated stretched sheet were examined by Makinde and Aziz (2011). They monitored that the characteristics of thermal can be considerably changed by mounting the effects of thermophoresis as well as Brownian motion. Rana and Bhargava (2012) inspected the steady flow holding nanoparticles past a non-linear stretched surface and obtained results numerically. Rashidi *et al.* (2013) considered electrically conducting flow containing nanoparticles using the second law of thermodynamics over a permeable rotating disk. The impact of heat generation on free convection flow containing nanofluid over a vertical surface immersed in non-Darcy medium was investigated by Chamkha *et al.* (2014). Beg *et al.* (2014) obtained the numerical results of single- and two-phase models in a circular tube filled with Al_2O_3–water based nanofluid. Garoosi *et al.* (2015) investigated free and mixed convective flow of a three types of nanofluid, namely, Cu, Al_2O_3 and TiO_2 in a cavity. Abolbashari *et al.* (2015) explored the outcome of partial slip on flow of a non-Newtonian Casson nanofluid toward a convectively heated stretched sheet with entropy generation and acquired the result via optimal homotopy technique. Free convective flow and heat exchangers in a cavity of nanofluid via the Buongiorno model containing various heaters and coolers was scrutinized by Garoosi *et al.* (2015). Freidoonimehr *et al.* (2015) calculated the MHD unsteady free convective flow of four different water-based nanofluids toward a porous vertical stretched sheet and

obtained the numerical solution via the shooting method with the RK technique. Rehman *et al.* (2016) investigated the Brownian motion and thermophoresis diffusion using the second law of thermodynamics of a non-Newtonian Jeffrey nanofluid over a stretched sheet with zero flux. The characteristics of three dimensional MHD flow of a non-Newtonian Carreau fluid past a stretched surface containing nanoparticles in the presence of thermal radiation was explored by Rudraswamy *et al.* (2017). Krishnamurthy *et al.* (2018) discussed the impact of Al_2O_3–water nanoparticle on flow with heat transfer past a stretched surface embedded in a porous medium with thermal radiation holding dust particles. Recently, Hayat *et al.* (2018a) explored the influence of entropy generation on mixed convective flow of water-based silver and copper nanoparticles via a rotating disk in the presence of viscous dissipation, thermal radiation and Joule heating.

The study of boundary layer flow with non-linear radiation and convective condition is considered in several engineering and industrial processes involving die forging, thermal energy storage, chemical reactions, gas and nuclear turbines. Aziz (2009) inspected the flow toward a heated flat surface. Makinde and Aziz (2010) scrutinized mixed convective flow and MHD heat transfer past a vertical heated plate immersed in porous medium. Yao *et al.* (2011) obtained an exact result for viscous flow toward a porous convectively heated stretched/shrinking wall. The viscous flow with heat transfer toward a porous stretched surface through convective conditions was investigated numerically by Ishak (2014). The effect of nonlinear radiation on stagnation point flow of nanofluid toward a stretched sheet through convective condition was studied numerically by Mushtaq *et al.* (2014). Rahman *et al.* (2015) studied mixed convection flow over a vertical heated flat surface. Mustafa *et al.* (2015) investigated the steady flow a Maxwell fluid over a heated exponentially stretched sheet immersed in a nanofluid. Ibrahim and Haq (2016) studied the MHD flow holding nanoparticles near a stagnation-point over a heated stretched sheet. Makinde *et al.* (2017) scrutinized MHD stagnation-point flow past a connective heated stretched sheet by slip and radiation effects comprising nanofluid. Khan *et al.* (2016) deliberated the effect of nonlinear radiation on MHD flow of a Carreau fluid past a nonlinear stretched sheet with convective boundary condition. The thermal conductivity dependence on temperature near a stagnation-point toward a non-linear stretching sheet in the presence of variable thickness with Cattaneo–Christov heat flux was scrutinized by Hayat *et al.* (2016a). In another paper, Hayat *et al.* (2016b) discussed the influences of homogenous–heterogeneous reactions on stagnation-point flow of a Maxwell fluid past a stretched cylinder with the Cattaneo–Christov heat flux. Mabood and Khan (2016) obtained the analytic solution of the MHD unsteady flow over a convectively heated stretched sheet holding nanoparticles. The influence of radiative flow on Oldroyd-B two-phase flow over a cone/wedge with Cattaneo–Christov heat flux was discussed by Reddy *et al.* (2018). Hayat *et al.* (2018b) discussed combined effects of Joule heating and viscous dissipation on radiative flow via a rotating disk in the presence of a magnetic field.

The objective of the current research is to study the nonlinear radiative heat transfer on flow by dispersing nanoparticles into non-Newtonian Williamson fluid past a heated unsteady shrinking sheet. The transformed nonlinear differential equations are numerically solved via shooting technique. Multiple solutions are obtained for accelerating flow and definite values of suction parameter. To the best of the authors' knowledge, no one yet has considered this type of problem. We expected that the present outcomes will give significant information for researchers. It is renowned that several devices meet flat or unexpected alteration in the environment of aerodynamic. The rotor of helicopter, the propeller of ship, etc., normally operate in an unsteady environment.

2. Mathematical formulation

Consider an unsteady nonlinear radiative flow of a non-Newtonian Williamson fluid toward a porous convectively heated shrinking surface filled with nanoparticles. It is presumed that $\ddot{x}-$, $\ddot{y}-$ axes measured along the shrinking surface and normal to it, respectively. It is also supposed that the velocity of surface is $\ddot{u}_w(\ddot{x},\ddot{t}) = -a\ddot{x}/(1-c\ddot{t})$ with $a(>0)$ and c are constants with dimensions $\mathbf{T^{-1}}$(see Figure 1). Further, it is assumed that at lower surface, the sheet was heated convectively with temperature $\ddot{T}_f$ that offers a coefficient of heat transfer h_f. For Williamson fluid, the stress-tensor is specified as (Nadeem *et al.*, 2013)

$$\ddot{S} = -\ddot{p}I + \ddot{\varepsilon}, \tag{1}$$

and

$$\ddot{\varepsilon} = \left(\ddot{\mu}_\infty + \frac{\ddot{\mu}_0 - \ddot{\mu}_\infty}{1-\ddot{\Gamma}\dot{\alpha}}\right)\ddot{A}_1, \tag{2}$$

where $\ddot{\varepsilon}$, $\ddot{\mu}_0$ and $\ddot{\mu}_\infty$are extra stress tensor, limiting viscosities at zero and infinite shear stress, respectively, $\ddot{\Gamma} > 0$ time constant, A_1 the first Rivilin–Erickson tensor and $\dot{\alpha}$is described as:

$$\dot{\alpha} = \sqrt{\frac{1}{2}\pi}, \quad \pi = \text{trace}\left(\ddot{A}_1^2\right) \tag{3}$$

Now, we only consider the case in which.

Figure 1 Sketch of the physical flow problem

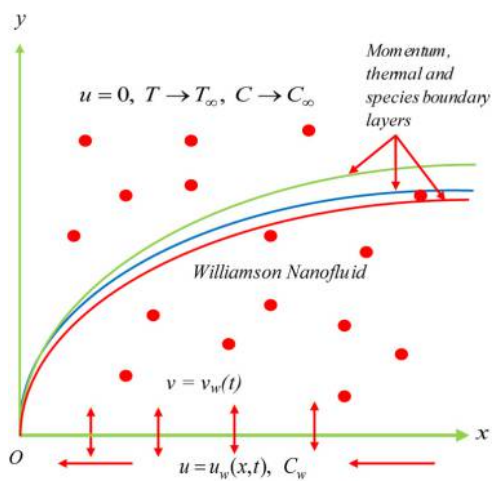

$$\ddot{\mu}_\infty = 0,\ \ddot{\Gamma}\dot{\alpha} < 1.$$

Thus, we get

$$\varsigma = \frac{\ddot{\mu}_0}{1-\ddot{\Gamma}\dot{\alpha}}\ddot{A}_1 \tag{4}$$

Or using binomial expansion:

$$\varsigma = \ddot{\mu}_0(1+\ddot{\Gamma}\dot{\alpha})\ddot{A}_1 \tag{5}$$

Under these assumptions, the physical equations that govern the unsteady flow are written as (Kumar *et al.*, 2017b; Srinivas *et al.*, 2017):

$$\frac{\partial \ddot{u}}{\partial \ddot{x}} + \frac{\partial \ddot{v}}{\partial \ddot{y}} = 0, \tag{6}$$

$$\frac{\partial \ddot{u}}{\partial \ddot{t}} + \ddot{u}\frac{\partial \ddot{u}}{\partial \ddot{x}} + \ddot{v}\frac{\partial \ddot{u}}{\partial \ddot{y}} = \nu\frac{\partial^2 \ddot{u}}{\partial \ddot{y}^2} + \sqrt{2}\nu\ddot{\Gamma}\frac{\partial \ddot{u}}{\partial \ddot{y}}\frac{\partial^2 \ddot{u}}{\partial \ddot{y}^2}, \tag{7}$$

$$\frac{\partial \ddot{T}}{\partial \ddot{t}} + \ddot{u}\frac{\partial \ddot{T}}{\partial \ddot{x}} + \ddot{v}\frac{\partial \ddot{T}}{\partial \ddot{y}} = \ddot{\alpha}\frac{\partial^2 \ddot{T}}{\partial \ddot{y}^2} + \ddot{\tau}\left[D_B\frac{\partial \ddot{C}}{\partial \ddot{y}}\frac{\partial \ddot{T}}{\partial \ddot{y}} + \left(\frac{D_T}{\ddot{T}_\infty}\right)\left(\frac{\partial \ddot{T}}{\partial \ddot{y}}\right)^2\right] - \frac{1}{(\rho c_p)_f}\frac{\partial q_r}{\partial \ddot{y}}, \tag{8}$$

$$\frac{\partial \ddot{C}}{\partial \ddot{t}} + \ddot{u}\frac{\partial \ddot{C}}{\partial \ddot{x}} + \ddot{v}\frac{\partial \ddot{C}}{\partial \ddot{y}} = D_B\frac{\partial^2 \ddot{C}}{\partial \ddot{y}^2} + \left(\frac{D_T}{\ddot{T}_\infty}\right)\left(\frac{\partial \ddot{T}^2}{\partial \ddot{y}^2}\right), \tag{9}$$

The boundary conditions are:

$$\begin{aligned}
&\ddot{t} < 0: \ddot{u} = 0,\ \ddot{v} = 0,\ \ddot{T} = \ddot{T}_\infty,\ \ddot{C} = \ddot{C}_\infty \text{ for all } \ddot{x}, \ddot{y},\\
&\ddot{t} \geq 0: \ddot{u} = \ddot{u}_w(\ddot{x}, \ddot{t}),\ \ddot{v} = -\ddot{v}_w(\ddot{t}),\ -k\frac{\partial \ddot{T}}{\partial \ddot{y}} = h_f(\ddot{t})\left(\ddot{T}_f - \ddot{T}\right),\\
&\ddot{C} = \ddot{C}_w \text{ at } \ddot{y} = 0,\ \ddot{u} \to 0,\ \ddot{T} \to \ddot{T}_\infty,\ \ddot{C} \to \ddot{C}_\infty \text{ as } \ddot{y} \to \infty.
\end{aligned} \tag{10}$$

where $\ddot{u}, \ddot{v}$ are velocity components in $\ddot{x}-$ and $\ddot{y}-$ axes, respectively, $\ddot{\alpha}$is the thermal diffusivity, ν is the kinematic viscosity, ρ is the density, $\ddot{T}$ is the temperature, $\ddot{T}_\infty$ is the free stream temperature, $\ddot{C}$ is the concentration of nanoparticles, D_B and D_T are the coefficients of Brownian and thermophoresis diffusion, respectively, $\ddot{\tau}$ is the ratio b/w the heat capacity and specific heat capacitance of nanoparticle material and the fluid and $(\rho c_p)_f$ the specific heat capacitance of nanofluid.

Following Khan *et al.* (2016), the heat flux of radiative q_r is communicated as:

$$\ddot{q}_r = -\frac{4\ddot{\sigma}^*}{3\ddot{k}^*}\frac{\partial \ddot{T}^4}{\partial \ddot{y}} = -\frac{16\ddot{\sigma}^*}{3\ddot{k}^*}\ddot{T}^3\frac{\partial \ddot{T}}{\partial \ddot{y}}, \tag{11}$$

where $\ddot{\sigma}^*$ the constant of Stefan–Boltzmann and $\ddot{k}^*$ the coefficient of mean absorption. Using equation (11), Energy equation (8) can be written as follows:

$$\frac{\partial \ddot{T}}{\partial \ddot{t}} + \ddot{u}\frac{\partial \ddot{T}}{\partial \ddot{x}} + \ddot{v}\frac{\partial \ddot{T}}{\partial \ddot{y}} = \frac{\partial}{\partial \ddot{y}}\left[\left(\ddot{\alpha} + \frac{16\ddot{\sigma}^*\ddot{T}^3}{3(\rho c_p)_f\ddot{k}^*}\right)\frac{\partial \ddot{T}}{\partial \ddot{y}}\right] + \ddot{\tau}\left[D_B\frac{\partial \ddot{C}}{\partial \ddot{y}}\frac{\partial \ddot{T}}{\partial \ddot{y}} + \left(\frac{D_T}{\ddot{T}_\infty}\right)\left(\frac{\partial \ddot{T}}{\partial \ddot{y}}\right)^2\right]. \tag{12}$$

Now, we introduce the similarity transformation (Naganthran *et al.*, 2016):

$$\eta = \ddot{y}\sqrt{\frac{a}{\nu(1-c\ddot{t})}},\ \psi = \sqrt{\frac{a\nu}{(1-c\ddot{t})}}\ddot{x}f(\eta),$$
$$\theta(\eta) = \frac{\ddot{T}-\ddot{T}_\infty}{\ddot{T}_f-\ddot{T}_\infty},\ \phi(\eta) = \frac{\ddot{C}-\ddot{C}_\infty}{\ddot{C}_w-\ddot{C}_\infty}. \tag{13}$$

Here η, ψ is the similarity variable and the stream function, respectively. We get $\ddot{T} = \ddot{T}_\infty[1+(\theta_w-1)\theta]$, with $\theta_w > 1$, where $\theta_w = \ddot{T}_f/\ddot{T}_\infty$ being the temperature ratio parameter. Here for similarity solution, we assumed that $\ddot{\Gamma} = \ddot{\Gamma}_1(1-c\ddot{t})^{3/2}/\ddot{x}$ (Naganthran *et al.*, 2016), $\ddot{v}_w(\ddot{t}) = v_0/\sqrt{1-c\ddot{t}}$ the variable velocity of suction with v_0 a positive constant and $h_f(\ddot{t}) = d/\sqrt{1-c\ddot{t}}$ with $d > 0$ (Mahapatra and Nandy, 2013).

In view of relation (13), equations (7)-(12) are transmuted into ODEs:

$$f''' + ff'' - f'^2 + \delta f''f''' - A\left(f' + \frac{1}{2}\eta f''\right) = 0, \tag{14}$$

$$\theta'' + \mathrm{Pr}f\theta' + \frac{4}{3R_d}\frac{d}{d\eta}\left[\{1+(\theta_w-1)\theta\}^3\theta'\right] + \mathrm{Pr}\left[Nb\theta'\phi' + Nt(\theta')^2\right] - \frac{1}{2}\mathrm{Pr}A\eta\theta' = 0, \tag{15}$$

$$\phi'' + Scf\phi' + \frac{Nt}{Nb}\theta'' - \frac{1}{2}\mathrm{Pr}\,ScA\eta\phi' = 0, \tag{16}$$

Subject to the boundary conditions:

$$f(0) = S,\ f'(0) = -1,\ \theta'(0) = -\gamma(1-\theta(0)),\ \phi(0) = 1,$$
$$f'(\infty) \to 0,\ \theta(\infty) \to 0,\ \phi(\infty) \to 0. \tag{17}$$

where prime signifies differentiation w.r.t η, $\delta = \sqrt{2}\Gamma_1 a^{3/2}/\sqrt{\nu}$ the non-Newtonian Williamson parameter, $A = c/a$ an unsteady parameter, $\mathrm{Pr} = \ddot{\nu}/\ddot{\alpha}$ the Prandtl number, $Nb = \ddot{\tau}D_B(\ddot{C}_w - \ddot{C}_\infty)/\ddot{\nu}$ the Brownian motion parameter, $Nt = \ddot{\tau}D_T\left(\ddot{T}_f - \ddot{T}_\infty\right)/\ddot{T}_\infty\ddot{\nu}$ the thermophoresis parameter, $\gamma = d\sqrt{\ddot{\nu}/a}/k$ the convective parameter, $R_d = \ddot{k}\ddot{k}^*/4\ddot{\sigma}^*\ddot{T}_\infty^3$ the thermal radiation parameter, $S = v_0/\sqrt{a\nu} > 0$ the suction parameter and $Sc = \nu/D_B$ the Schmidt number.

The vital physical quantities are the skin friction coefficient; the Nusselt and the Sherwood numbers are defined as follows:

$$\ddot{C}_f = \frac{\ddot{\tau}_w}{\rho\ddot{u}_w^2},\ Nu_x = -\frac{\ddot{x}\ddot{q}_w}{\ddot{k}\left(\ddot{T}_f - \ddot{T}_w\right)},\ Sh\ddot{x} = \frac{\ddot{x}\ddot{m}_w}{D_B(\ddot{C}_w - \ddot{C}_\infty)}, \tag{18}$$

where $\ddot{\tau}_w, \ddot{q}_w, \ddot{m}_w$ the shear stress in $\ddot{x}-$ direction, the heat and the mass fluxes, respectively, which are given as:

$$\ddot{\tau}_w = \ddot{\mu}_0\left(\frac{\partial \ddot{u}}{\partial \ddot{y}} + \frac{\ddot{\Gamma}}{\sqrt{2}}\left(\frac{\partial \ddot{u}}{\partial \ddot{y}}\right)^2\right)_{\ddot{y}=0},$$
$$\ddot{q}_w = -\ddot{k}\left(\frac{\partial \ddot{T}}{\partial \ddot{y}}\right)_w + (\ddot{q}_r)_w,\ \ddot{m}_w = -D_B\left(\frac{\partial \ddot{C}}{\partial \ddot{y}}\right)_{\ddot{y}=0}, \tag{19}$$

Using (13), we get:

$$C_f \mathrm{Re}_x^{1/2} = f''(0) + \frac{\delta}{2}\left(f''(0)\right)^2, \; Sh_x \mathrm{Re}_x^{-1/2} = -\phi'(0),$$
$$Nu_x \mathrm{Re}_x^{-1/2} = -\left[1 + \frac{4}{3R_d}\left\{1 + (\theta_w - 1)\theta(0)\right\}^3\right]\theta'(0). \tag{20}$$

where $\mathrm{Re}_x = \dot{x}\dot{u}_w(\dot{x}, \dot{t})/\dot{\nu}$ is the Reynolds number.

3. Methodology

In the present research, a useful numerical technique, namely, the shooting method has been used to scrutinize the flow problem described by the transformed equations (14)-(17). The summary of this method is given below in following steps:

First, convert equations (14)-(17) into initial value problem (IVP). Then select a suited finite value of $\eta \to \infty$, say, η_∞. We have the set of following first-order system:

$$\left.\begin{aligned} f' &= p, \\ p' &= q, \\ q' &= \left(p^2 - fq - 1 - K(1-p) - \lambda\theta\right)/\Lambda\left(1 + \frac{1}{\beta_1}\right), \end{aligned}\right\} \tag{21}$$

$$\left.\begin{aligned} \theta' &= z, \\ z' &= \begin{pmatrix} -\mathrm{Pr}fz - \frac{4}{R_d}(\theta_w - 1)\left\{1 + (\theta_w - 1)\theta\right\}^2 z^2 \\ -\mathrm{Pr}(Nbzm + Ntz^2) + \frac{1}{2}\mathrm{Pr}A\eta z \end{pmatrix} \Big/ \left(1 + \frac{4}{3R_d}\left\{1 + (\theta_w - 1)\theta\right\}^3\right), \end{aligned}\right\} \tag{22}$$

$$\left.\begin{aligned} \phi' &= m, \\ m' &= -Scfm - \frac{Nt}{Nb}z' + \frac{1}{2}ScA\eta m, \end{aligned}\right\} \tag{23}$$

Under the boundary conditions:

$$f(0) = S,\; p(0) = -1,\; z(0) = -\gamma(1 - \theta(0)),\; \phi(0) = 1. \tag{24}$$

To solve the system of equations as an IVP, we require the values for $q(0)$ i.e. $f'(0)$, $z(0)$ i.e. $\theta'(0)$ and $m(0)$ i.e. $\phi'(0)$; however, no such values are specified. The values of the initial guesses for $f'(0)$, $\theta'(0)$ and $\phi'(0)$ are chosen, and the Runge–Kutta fourth-order method is executed to acquire a solution. Then, the calculated values of $f'(\eta)$, $\theta(\eta)$ and $\phi(\eta)$ at η_∞ (=8) are compared under the known boundary conditions $f'(\eta_\infty) = 0$, $\theta(\eta_\infty) = 0$ and $\phi(\eta_\infty) = 0$. The step size is taken as $\Delta\eta = 0.01$. The technique is repeated until we obtain results correct up to the desired accuracy of the 10^{-5} level, which fulfills the convergence criterion.

4. Results and discussion

Tables I and II show the assessment of our results of $-f'(0)$ and $-\theta'(0)$, respectively, with those available results in literature. As noticed an excellent match with the published ones up to a significant number of digits has been obtained.

The velocity, temperature distribution and the concentration of nanoparticles for different values of the non-Newtonian Williamson parameter δ are depicted in Figures 2-4. From Figure 2, the velocity explains a diminishing development for growing values of δ in the first solution. and thus, the

Table I Comparison of $-f'(0)$ when $\delta = 0$ (Newtonian fluid), $S = 0$ in case of stretching sheet $f'(0) = 1$

A	Sharidan *et al.* (2006)	Chamkha *et al.* (2010)	Present
0.8	1.261042	1.261512	1.2610
1.2	1.377722	1.378052	1.3777

Table II Comparison of $-\theta'(0)$ when $\delta = 0$ (Newtonian fluid), $S = 0$, $R_d \to \infty$, Pr = 10, $Sc = 10$, $\gamma = 0.1$ in case of stretching sheet $f'(0) = 1$

Nt	Nb	Makinde and Aziz (2011)	Present
0.1	0.1	0.0929	0.0929
	0.2	0.0873	0.0873
0.2	0.1	0.0927	0.0927
	0.2	0.0868	0.0868
0.3	0.1	0.0925	0.0925
	0.2	0.0861	0.0861
0.4	0.1	0.0923	0.0923
	0.2	0.0854	0.0854
0.5	0.1	0.0921	0.0921
	0.2	0.0845	0.0845

Figure 2 The velocity profiles for different values of δ

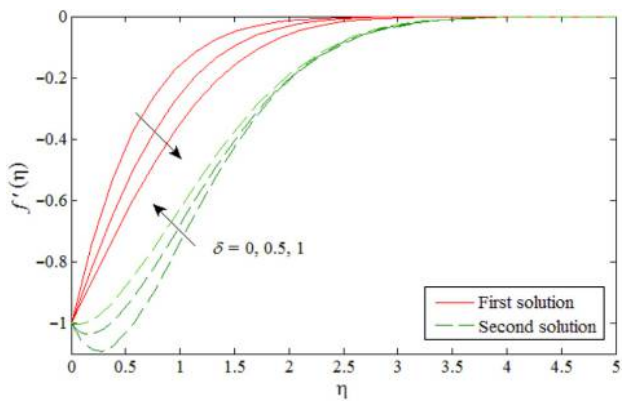

Figure 3 The temperature profiles for different values of δ

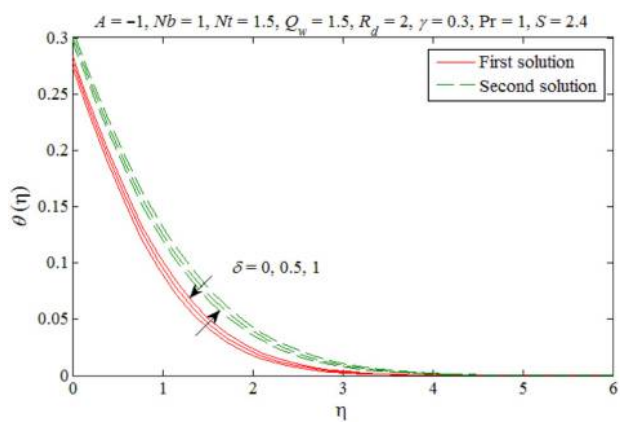

Figure 4 The concentration profiles for different values of δ

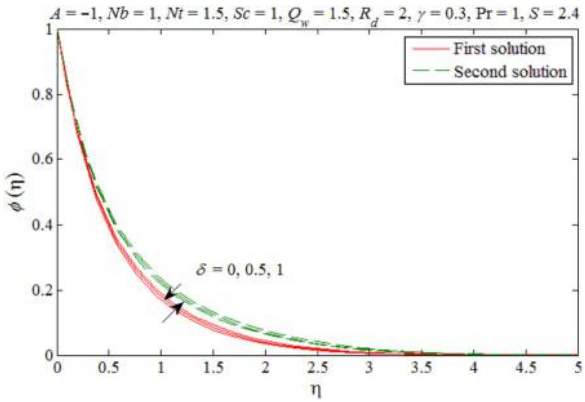

momentum boundary layer thickness increases, while the velocity enhances and the boundary thickness decreases in the second solution. In contrast, the temperature distribution and the concentration of nanoparticles show an increasing behavior with increasing values of δ for the first solution, as portrayed in Figures 3 and 4, and consequently, the thermal and concentration boundary layers thicknesses boost. On the other hand, for the second solution, the reverse trend is observed. It is also witnessed from these portrays that the velocity, temperature distribution and the concentration of nanoparticles are larger for a non-Newtonian Williamson fluid compared with a Newtonian fluid ($\delta = 0$) for the first solution.

Figures 5-7 preserve the variation of unsteady parameter A on the velocity of fluid, temperature distribution and concentration of nanoparticles. Figure 5 indicates an increasing trend in velocity field with rising values of A in the first solution, and in the second solution, the profile indicates an opposite behavior. Further, it is also perceived from this portray that the velocity initially increases with increasing η for first solution and after a certain value of $\eta = 1$, it starts decreasing. The unsteady effect is major in the lower branch solution (second solution) compared to the upper branch solution (First solution). The temperature distribution and concentration profile increase with increasing A for first and second solutions, as shown in Figures 6 and 7, respectively. Thus, the thermal and concentration boundary layers thicknesses increase for

Figure 5 The velocity profiles for different values of A

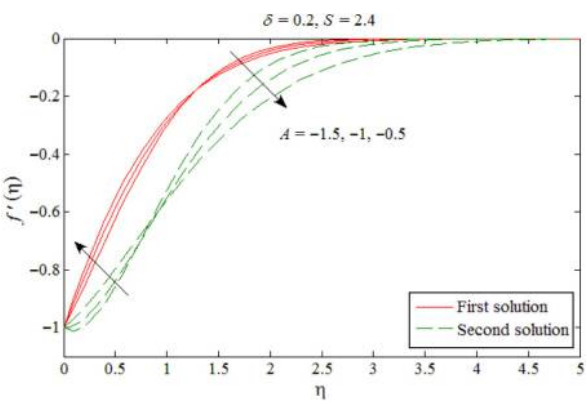

Figure 6 The temperature profiles for different values of A

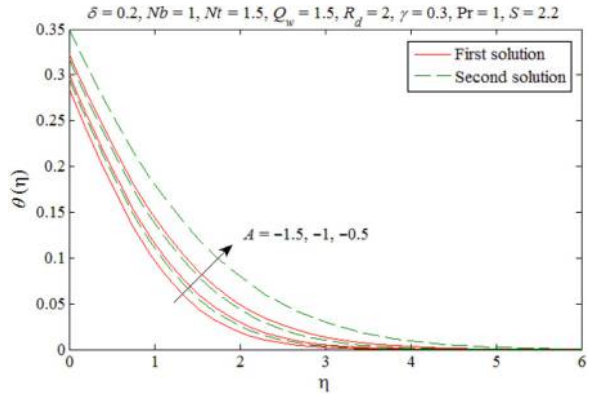

Figure 7 The concentration profiles for different values of A

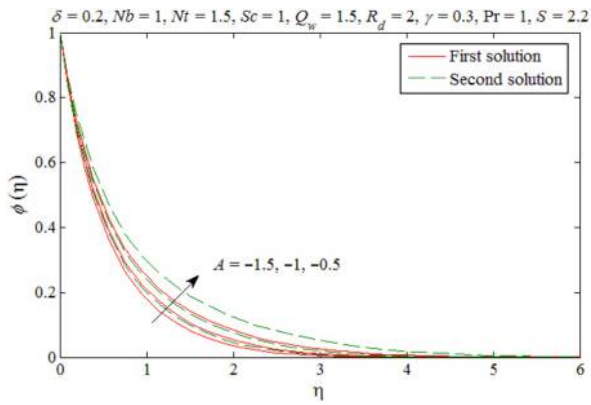

both solutions. Further, these sketches fulfill asymptotically the boundary conditions and the existence of multiple solutions that support the validation of our obtained numerical results.

Figure 8 shows that owing to mounting values of the Brownian parameter Nb, the temperature distribution raises in the first and second solutions, whereas the conflicting behavior is noticed for the concentration of nanoparticle, as revealed in Figure 9. Thus, the thermal boundary layer thickness increases,

Figure 8 The temperature profiles for different values of Nb

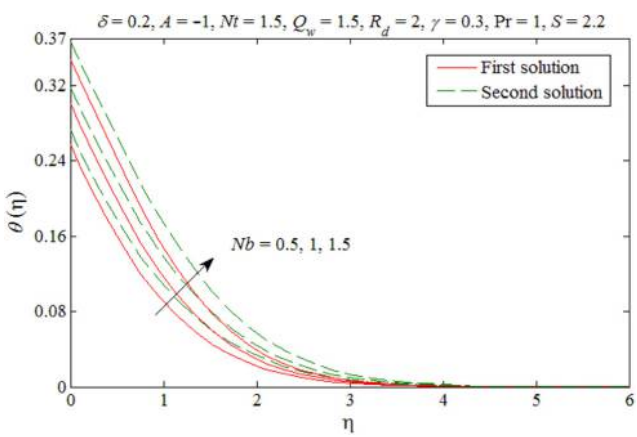

Figure 9 The concentration profiles for different values of *Nb*

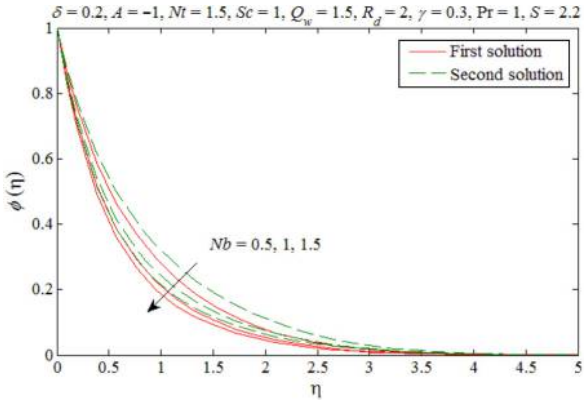

while the concentration boundary layer thickness shrinks. This is because of the kinetic energy of the nanoparticles increases owing to the strength of this chaotic motion, and as a result, the fluids temperature increases. This is because the Brownian motion at nanoscale and molecular levels is an important mechanism of the nanoscale level that governs the thermal behaviors. In systems using nanofluids, the Brownian motion captures place because of the nanoparticles size, which can change the properties of heat transfer. As the scale size of particles advances to the scale of nanometer, the particles Brownian motion, and its result on the surrounding fluids play a vital role in heat transfer characteristics. Figures 10 and 11 preserve the influence of the thermophoresis parameter *Nt* on the temperature distribution and concentration profile. These figures illustrate that the temperature and concentration profiles show an increasing trend for increasing values of *Nt* for first as well as for second solutions. This is because diffusion penetrates deeper into the fluid owing to increasing values of *Nt* which causes the thickening of the thermal boundary layer as well as the concentration boundary layer.

The effects of the convective parameter γ on the temperature distribution and concentration of nanoparticles are depicted in Figures 12 and 13, respectively. Figure 12 reveals that owing to increase in the value of γ resulting from the powerful convective heating at the surface, the temperature gradient at the surface of sheet increases. This permits the effect of thermal

Figure 10 The temperature profiles for different values of *Nt*

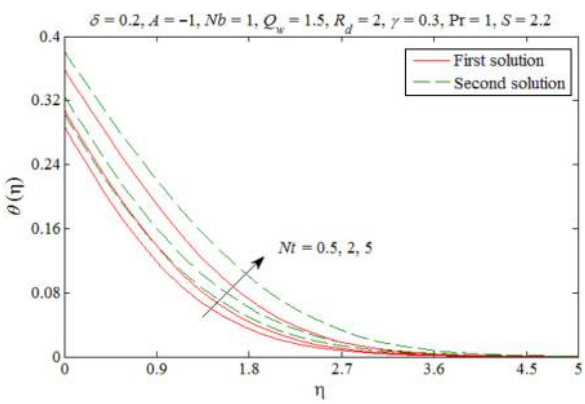

Figure 11 The concentration profiles for different values of *Nt*

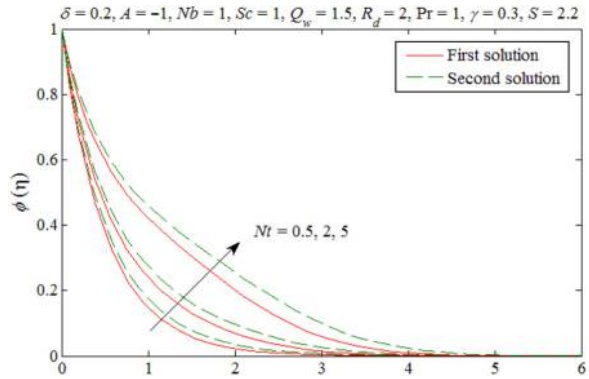

Figure 12 The temperature profiles for different values of γ

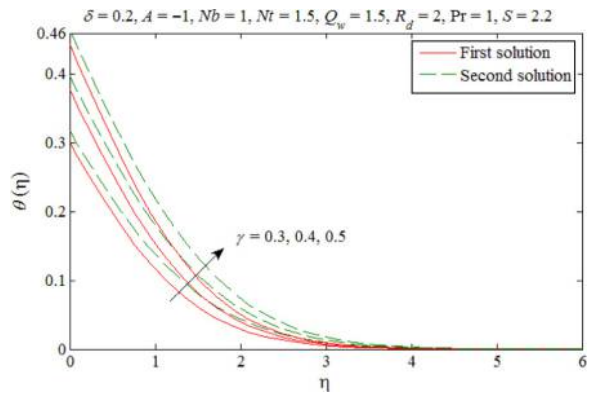

Figure 13 The concentration profiles for different values of γ

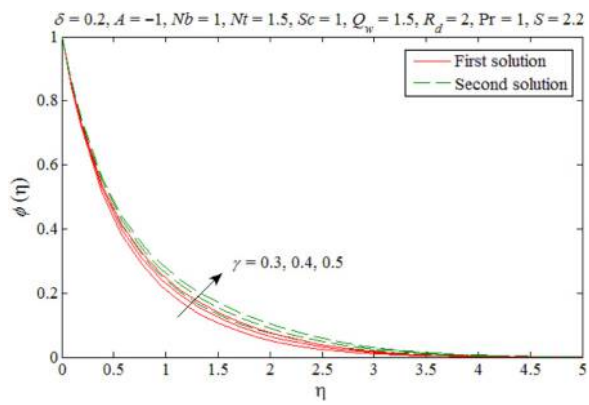

to enter deeper into the quiescent fluid. Therefore, the temperature as well as the thermal boundary layer thickness enhances with rising values of γ for first and second solutions. It is worth mentioning that the constant wall temperature $\theta(0) = 1$ can be recovered by taking sufficiently large values of the convective parameter. Further $\gamma = 0$ communicates an insulated surface case. Figure 13 confirms that the concentration of nanoparticles and the boundary layer thickness increase with γ in the first and second solutions. Figures 14 and 15 are prepared to illustrate the impact of

Figure 14 The temperature profiles for different values of R_d

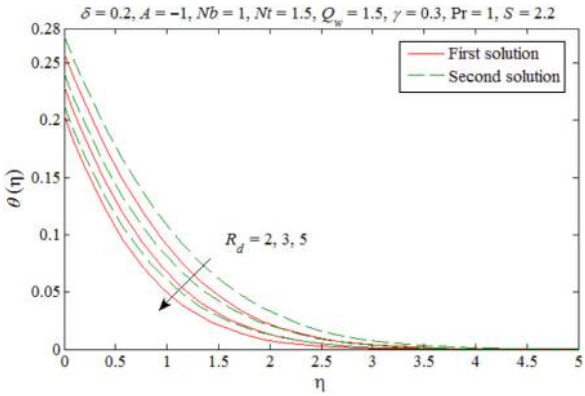

Figure 15 The concentration profiles for different values of R_d

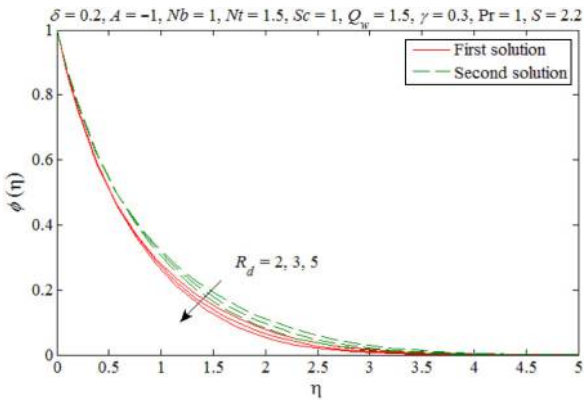

radiation R_d on temperature distribution and concentration nanoparticles. These figures showed a decreasing behavior for increasing R_d in the first and second solutions. Thus, the thermal and concentration boundary layers thicknesses become thinner and thinner in both forms. A huge value of the radiation means the conduction dominance and, thus, the thermal and concentration boundary layers thicknesses decrease. The impact of radiation is more pronounced on temperature distribution compared to concentration profile. In Figure 16, the Schmidt number effect on the concentration of nanoparticles is shown. As expected, the graph and the boundary layer thickness shrinks with enhancing Sc in the first and second solutions.

Figure 16 The concentration profiles for different values of Sc

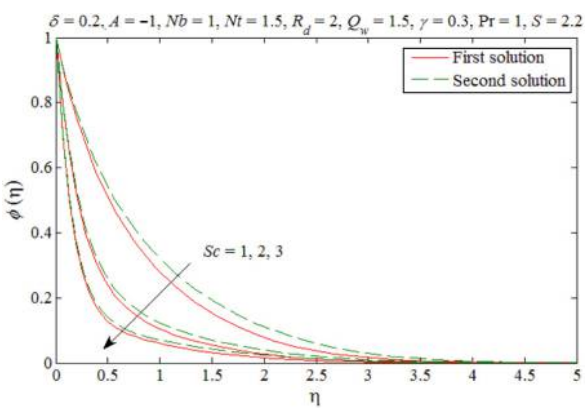

The impact of the non-Newtonian Williamson fluid parameter δ versus A on the skin friction, the local Nusselt and Sherwood numbers are shown in Figures 17-19. It can be seen that multiple solutions of the similarity equations (14)-(16)

Figure 17 The skin friction $C_f \mathrm{Re}_x^{1/2}$ versus A for different values of δ

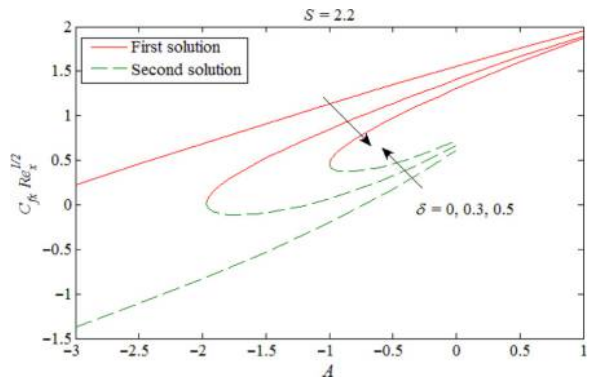

Figure 18 The Nusselt number $Nu_x \mathrm{Re}_x^{-1/2}$ versus A for different values of δ

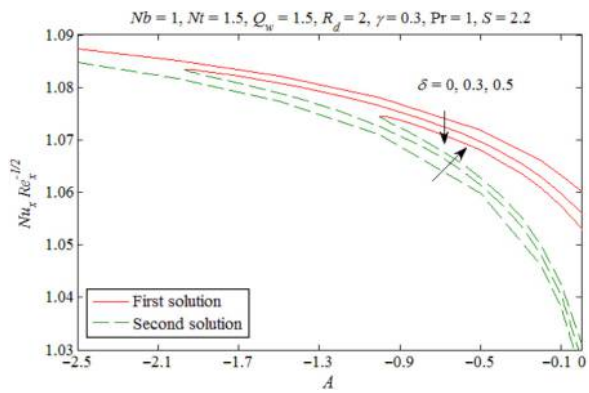

Figure 19 The Sherwood number $Sh_x \mathrm{Re}_x^{-1/2}$ versus A for different values of δ

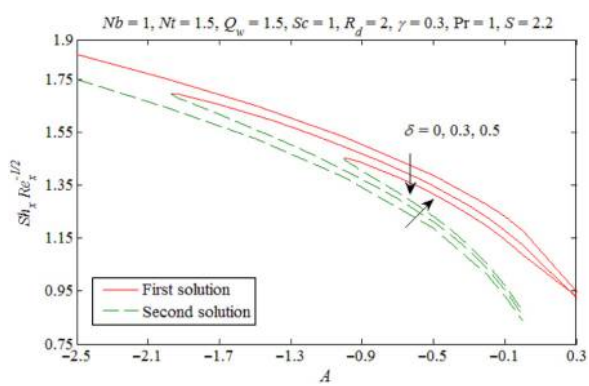

subjected to (17) exist in decelerating flow ($A \leq 0$; see Mahapatra and Nandy, 2013), while for accelerating flow ($A > 0$), the solution is unique. On the other hand, the dual solutions are obtained for $A \geq A_c$ and the flow has no solution for $A < A_c$, where A_c is the critical value of A. For $\delta = 0$ (Newtonian fluid), the critical point looks far from negative region, so we stopped calculation at $A = -10$. This is consistent with the results obtained in References (Ali *et al.*, 2011; Rohni, 2012). For $\delta = 0.3$, the dual solutions exist for ranges of A is $A \geq -1.9700$, and thus, no solution exists for $A < -1.9700$. It is worth mentioning that more amount of non-Newtonian parameter δ causes a remarkable reduction ($|A_c|$) in the solution domain. For $\delta = 0.5$, the solution exists when $A \geq -1.0000$, and therefore, no solution exists for A < -1.0000. Thus, it can be concluded that the critical point ($|A_c|$) reduces when non-Newtonian parameter increases, which delays the boundary layer separation. Further, owing to increasing values of δ, the skin friction, the local Nusselt and Sherwood numbers decrease for the first solution and increases in case of second solution, as illustrated in Figures 17-19.

The values $C_f \mathrm{Re}_x^{1/2}$, $Nu_x \mathrm{Re}_x^{-1/2}$ and $Sh_x \mathrm{Re}_x^{-1/2}$ versus S for several values of the unsteady parameter A are illustrated in Figures 20-22, respectively, and in Table III. Figure 20 reveals that the skin friction enhances with increasing A for the first as well as the second solutions. In contrast, the values of the Nusselt and Sherwood numbers decrease with increasing A for

Figure 20 The skin friction $C_f \mathrm{Re}_x^{1/2}$ versus S for different values of A

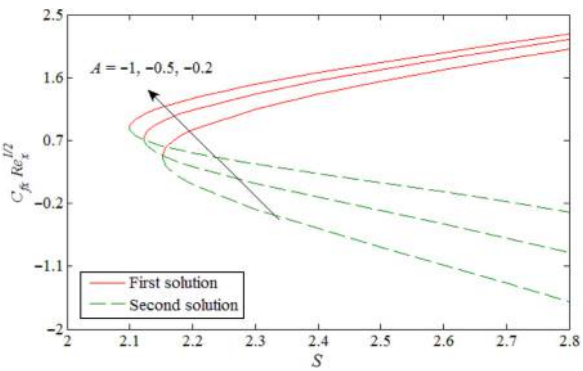

Figure 21 The Nusselt number $Nu_x \mathrm{Re}_x^{-1/2}$ versus S for different values of A

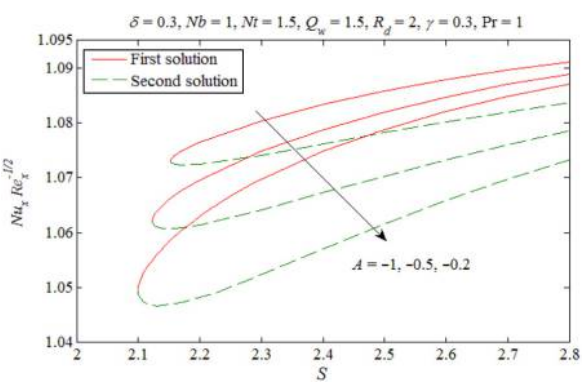

Figure 22 The Sherwood number $Sh_x \mathrm{Re}_x^{-1/2}$ versus S for different values of A

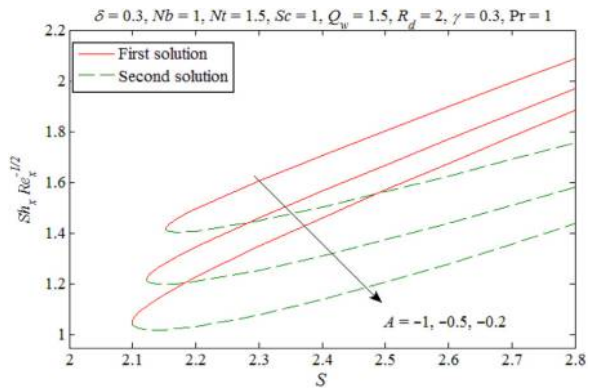

the first and second solutions, as shown in Figures 21 and 22. The behavior of these results also can be seen through Table II. Dual solutions are achieved for $S \geq S_c$, and no solution for $S < S_c$, where S_c is the critical value of S. Further, the impact of A toward a critical value has been shown in Table IV. The larger characteristics of unsteady parameter decrease the values of critical point. Thus, the unsteady parameter delays the boundary layer separation.

Figures 23 and 24 confirm the deviations of the Nusselt number $Nu_x \mathrm{Re}_x^{-1/2}$ and the Sherwood number $Sh_x \mathrm{Re}_x^{-1/2}$ versus S for different values of the Brownian motion parameter Nb. These results prove that the values of the Nusselt number decreases and the Sherwood number increases with enlarging Nb in the first and second solutions. These results are consistent with the results obtained by Rana and Bhargava (2012) in the case of a nonlinearly stretching sheet. Therefore, by using the Brownian motion, the thermal conduction can be increased either by taking straight outcome owing to nanoparticles that transport heat or by taking indirect micro-convection of the surrounding fluid individual nanoparticles. Further, the smaller values of Nb indicate that the Brownian motion is weak for the small particles and for larger values of Nb it shows the opposite behavior.

5. Conclusions

In this research, we have investigated unsteady boundary layer flow of non-Newtonian Williamson nanofluid over a convectively heated shrinking sheet with a nonlinear thermal radiation. The transformed ordinary differential equations were numerically solved via the shooting technique for several values of the pertinent parameters. The main findings are as follows:

- multiple results are achieved for some values of the suction and for decelerating flow only;
- owing to the non-Newtonian parameter, the velocity of the fluid decreases in the first solution and increases in the second solution. On the other hand, the temperature and concentration profiles increase and decrease in the first and the second solutions, respectively;
- initially, the velocity distribution shows an increasing behavior and then it starts to decrease owing to increasing values of the unsteady parameter for both solutions, while

Table III Values of skin friction, Nusselt number and Sherwood number versus S for different values of a when $\delta = 0.3$, $Nb = 1$, $Nt = 1.5$, $Sc = 1$, $Q_w = 1.5$, $R_d = 2$, $\gamma = 0.3$ are fixed

		$C_f Re_x^{1/2}$		$Nu_x Re_x^{-1/2}$		$Sh_x Re_x^{-1/2}$	
S	A	First solution	Second solution	First solution	Second solution	First solution	Second solution
2.8	−1	2.0069	−1.6142	1.0911	1.0837	2.0890	1.7582
	−0.5	2.1436	−0.9050	1.0889	1.0785	1.9692	1.5839
	−0.2	2.2258	−0.3232	1.0871	1.0733	1.8844	1.4394
2.4	−1	1.3650	−0.5630	1.0833	1.0762	1.7062	1.5043
	−0.5	1.5551	−0.1125	1.0788	1.0673	1.5666	1.3116
	−0.2	1.6687	0.2284	1.0748	1.0570	1.4615	1.1399
2.2	−1	0.8513	0.0694	1.0765	1.0725	1.4969	1.4049
	−0.5	1.1381	0.3225	1.0696	1.0614	1.3469	1.2109
	−0.2	1.3010	0.5207	1.0630	1.0482	1.2278	1.0344

Table IV Critical values of S_c for different values of a when $\delta = 0.3$, $Nb = 1$, $Nt = 1.5$, $Sc = 1$, $Q_w = 1.5$, $R_d = 2$, $\gamma = 0.3$ are fixed

A	S_c
−1	2.1528
−0.5	2.1229
−0.2	2.0990

Figure 23 The Nusselt number $Nu_x Re_x^{-1/2}$ versus S for different values of Nb

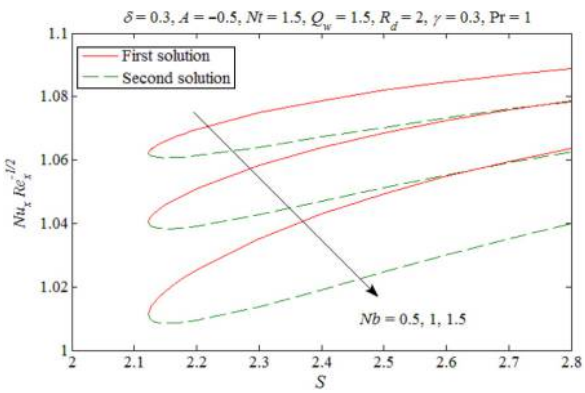

Figure 24 The Sherwood number $Sh_x Re_x^{-1/2}$ versus S for different values of Nb

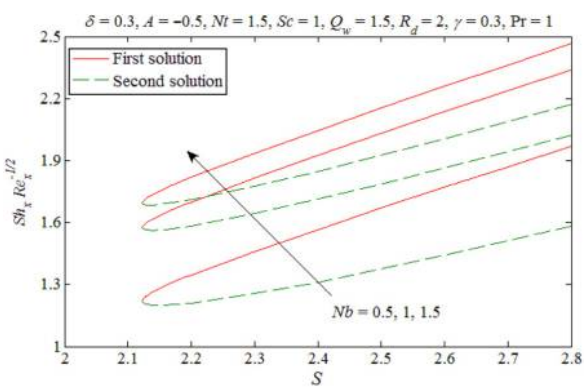

the temperature and concentration profiles confirm an increasing behavior in both solutions;

- the thermal and concentration boundary layer thicknesses develop owing to the convective parameter for the first and the second solutions;
- the thermal radiation reduces the temperature of the fluid as well as the concentration profile for both solutions;
- using the Brownian motion mechanism, the distribution of the nanoparticles could be arranged in the flow regime by taking larger values of Nb or Nt and also cooling of regime could be achieved by taking smaller values of Nb or Nt; and
- the unsteady parameter and the non-Newtonian parameter delay the boundary layer separation.

References

Abolbashari, M.H., Freidoonimehr, N., Nazari, F. and Rashidi, M.M. (2015), "Analytical modeling of entropy generation for Casson nano-fluid flow induced by a stretching surface", *Advanced Powder Technology*, Vol. 26 No. 2, pp. 542-552.

Ali, F.M., Nazar, R., Arifin, N.M. and Pop, I. (2011), "Unsteady flow and heat transfer past an axisymmetric permeable shrinking sheet with radiation effect", *International Journal for Numerical Methods in Fluids*, Vol. 67 No. 10, pp. 1310-1320.

Aziz, A. (2009), "A similarity solution for laminar thermal boundary layer over a flat plate with a convective surface boundary condition", *Communications in Nonlinear Science and Numerical Simulation*, Vol. 14 No. 4, pp. 1064-1068.

Beg, O.A., Rashidi, M.M., Akbari, M. and Hosseini, A. (2014), "Comparative numerical study of single-phase and two-Phase models for bio-nanofluid transport phenomena", *Journal of Mechanics in Medicine and Biology*, Vol. 14, pp. 1-31.

Buongiorno, J. (2006), "Convective transport in nanofluids", *Journal of Heat Transfer*, Vol. 128 No. 3, pp. 240-250.

Chamkha, A.J., Aly, A.M. and Mansour, M.A. (2010), "Similarity solution for unsteady heat and mass transfer from a stretching surface embedded in a porous medium with suction/injection and chemical reaction effects", *Chemical Engineering Communications*, Vol. 197 No. 6, pp. 846-858.

Chamkha, A.J., Rashad, A.M., Ram Reddy, Ch. and Murthy, P.V.S.N. (2014), "Effect of suction/injection on free

convection along a vertical plate in a nanofluid saturated non-Darcy porous medium with internal heat generation", *Indian Journal of Pure and Applied Mathematics*, Vol. 45 No. 3, pp. 321-342.

Freidoonimehr, N., Rashidi, M.M. and Mahmud, S. (2015), "Unsteady MHD free convective flow past a permeable stretching vertical surface in a nano-fluid", *International Journal of Thermal Sciences*, Vol. 87, pp. 136-145.

Garoosi, F., Bagheri, G. and Rashidi, M.M. (2015), "Two phase simulation of natural convection and mixed convection of the nanofluid in a square cavity", *Powder Technology*, Vol. 275, pp. 239-256.

Garoosi, F., Jahanshaloo, L., Rashidi, M.M., Badakhsh, A. and Ali, M.A. (2015), "Numerical simulation of natural convection of the nanofluid in heat exchangers using a buongiorno model", *Applied Mathematics and Computation*, Vol. 254, pp. 183-203.

Hayat, T., Ijaz Khan, M., Qayyum, S. and Alsaedi, A. (2018a), "Entropy generation in flow with silver and copper nanoparticles", *Colloids and Surfaces A: Physicochemical and Engineering Aspects*, Vol. 539, pp. 335-346.

Hayat, T., Qayyum, S., IjazKhan, M. and Alsaedi, A. (2018b), "Entropy generation in magnetohydrodynamic radiative flow due to rotating disk in presence of viscous dissipation and Joule heating", *Physics of Fluids*, Vol. 30 No. 1, pp. 017101.

Hayat, T., Ijaz Khan, M., Farooq, M., Yasmeen, T. and Alsaedi, A. (2016b), "Stagnation point flow with Cattaneo-Christov heat flux and homogeneous-heterogeneous reactions", *Journal of Molecular Liquids*, Vol. 220, pp. 49-55.

Hayat, T., Ijaz Khan, M., Farooq, M., Alsaedi, A., Waqas, M. and Yasmeen, T. (2016a), "Impact of Cattaneo–Christov heat flux model in flow of variable thermal conductivity fluid over a variable thicked surface", *International Journal of Heat and Mass Transfer*, Vol. 99, pp. 702-710.

Ibrahim, W. and Haq, R.U. (2016), "Magnetohydrodynamic (MHD) stagnation point flow of nanofluid past a stretching sheet with convective boundary condition", *Journal of the Brazilian Society of Mechanical Sciences and Engineering*, Vol. 38 No. 4, pp. 1155-1164.

Ishak, A. (2014), "Similarity solutions for flow and heat transfer over a permeable surface with convective boundary condition", *Applied Mathematics and Computation*, Vol. 217 No. 2, pp. 837-842.

Khan, N.A. and Khan, H.A. (2014), "Boundary layer flows of non-Newtonian Williamson fluid", *Nonlinear Engineering*, Vol. 3, pp. 107-115.

Khan, W.A. and Pop, I. (2010), "Boundary-layer flow of a nanofluid past a stretching sheet", *International Journal of Heat and Mass Transfer*, Vol. 53 Nos 11/12, pp. 2477-2483.

Khan, M., Hashim, Hussain, M. and Azam, M. (2016), "Magnetohydrodynamic flow of carreau fluid over a convectively heated surface in the presence of non-linear radiation", *Journal of Magnetism and Magnetic Materials*, Vol. 412, pp. 63-68.

Krishnamurthy, M.R., Kumar, K.G., Gireesha, B.J. and Rudraswamy, N.G. (2018), "MHD flow and heat transfer (PST and PHF) of dusty fluid suspended with alumina nanoparticles over a stretching sheet embedded in a porous medium under the influence of thermal radiation", *Journal of Nanofluids*, Vol. 7 No. 3, pp. 527-535.

Krishnamurthy, M.R., Prasannakumara, B.C., Gireesha, B.J. and Gorla, R.S.R. (2016), "Effect of chemical reaction on MHD boundary layer flow and melting heat transfer of Williamson nanofluid in porous medium", *Engineering Science and Technology, an International Journal*, Vol. 19 No. 1, pp. 53-61.

Kumar, K.G., Gireesha, B.J. and Gorla, R.S.R. (2018), "Flow and heat transfer of dusty hyperbolic tangent fluid over a stretching sheet in the presence of thermal radiation and magnetic field", *International Journal of Mechanics and Materials in Design*, Vol. 13 No. 2, pp. 1-11.

Kumar, K.G., Haq, R.U., Rudraswamy, N.G. and Gireesha, B.J. (2017a), "Effects of mass transfer on MHD three dimensional flow of a prandtl liquid over a flat plate in the presence of chemical reaction", *Results in Physics*, Vol. 7, pp. 3465-3471.

Kumar, K.G., Rudraswamy, N.G., Gireesha, B.J. and Manjunatha, S. (2017b), "Non linear thermal radiation effect on Williamson fluid with particle-liquid suspension past a stretching surface", *Results in Physics*, Vol. 7, pp. 3196-3202.

Mabood, F. and Khan, W.A. (2016), "Analytical study for unsteady nanofluid MHD flow impinging on heated stretching sheet", *Journal of Molecular Liquids*, Vol. 219, pp. 216-223.

Mahapatra, T.R. and Nandy, S.K. (2013), "Slip effects on unsteady stagnation-point flow and heat transfer over a shrinking sheet", *Meccanica*, Vol. 48 No. 7, pp. 1599-1606.

Makinde, O.D. and Aziz, A. (2010), "MHD mixed convection from a vertical plate embedded in a porous medium with a convective boundary condition", *International Journal of Thermal Sciences*, Vol. 49 No. 9, pp. 1813-1820.

Makinde, O.D. and Aziz, A. (2011), "Boundary layer flow of a nanofluid past a stretching sheet with a convective boundary condition", *International Journal of Thermal Sciences*, Vol. 50 No. 7, pp. 1326-1332.

Makinde, O.D., Khan, W.A. and Khan, Z.H. (2017), "Stagnation point flow of MHD chemically reacting nanofluid over a stretching convective surface with slip and radiative heat", *Proceedings of the Institution of Mechanical Engineers, Part E: Journal of Process Mechanical Engineering*, Vol. 232 No. 4, pp. 1-9.

Malik, M.Y. and Salahuddin, T. (2015), "Numerical solution of MHD stagnation point flow of williamson fluid model over a stretching cylinder", *International Journal of Nonlinear Sciences and Numerical Simulation*, Vol. 16, pp. 2015161-2015164.

Masuda, H., Ebata, A., Teramae, K. and Hishinuma, N. (1993), "Alteration of thermal conductivity and viscosity of liquid by dispersing ultra-fine particles", *Netsu Bussei*, Vol. 7 No. 4, pp. 227-233.

Mushtaq, A., Mustafa, M., Hayat, T. and Alsaedi, A. (2014), "Nonlinear radiative heat transfer in the flow of nanofluid due to solar energy: a numerical study", *Journal of the Taiwan Institute of Chemical Engineers*, Vol. 45 No. 4, pp. 1176-1183.

Mustafa, M., Khan, J.A., Hayat, T. and Alsaedi, A. (2015), "Simulations for Maxwell fluid flow past a convectively heated exponentially stretching sheet with nanoparticles", *AIP Advances*, Vol. 5 No. 3, pp. 037133.

Nadeem, S. and Hussain, S.T. (2014), "Heat transfer analysis of Williamson fluid over exponentially stretching

surface", *Applied Mathematics and Mechanics*, Vol. 35 No. 4, pp. 489-502.

Nadeem, S., Hussain, S.T. and Lee, C. (2013), "Flow of a Williamson fluid over a stretching sheet", *Brazilian Journal of Chemical Engineering* Vol. 30 No. 3, pp. 619-625.

Naganthran, K., Nazar, R. and Pop, I. (2016), "Unsteady stagnation-point flow and heat transfer of a special third grade fluid past a permeable stretching/shrinking sheet", *Scientific Reports*, Vol. 6, pp. 24632.

Nield, D.A. and Kuznetsov, A.V. (2009), "The Cheng–Minkowycz problem for natural convective boundary-layer flow in a porous medium saturated by a nanofluid", *International Journal of Heat and Mass Transfer*, Vol. 52 Nos 25/26, pp. 5792-5795.

Nield, D.A. and Kuznetsov, A.V. (2010), "Natural convective boundary-layer flow of a nanofluid past a vertical plate", *International Journal of Thermal Sciences*, Vol. 49 No. 2, pp. 243-247.

Rahman, M.M., Merkin, J.H. and Pop, I. (2015), "Mixed convection boundary-layer flow past a vertical flat plate with a convective boundary condition", *Acta Mechanica*, Vol. 226 No. 8, pp. 2441-2460.

Rehman, S.U., Haq, R.U., Khan, Z.H. and Lee, C. (2016), "Entropy generation analysis for non-Newtonian nanofluid with zero normal flux of nanoparticles at the stretching surface", *Journal of the Taiwan Institute of Chemical Engineers*, Vol. 63, pp. 226-236.

Rana, P. and Bhargava, R. (2012), "Flow and heat transfer of a nanofluid over a nonlinearly stretching sheet: a numerical study", *Communications in Nonlinear Science and Numerical Simulation*, Vol. 17 No. 1, pp. 212-226.

Rashidi, M.M., Abelman, S. and Freidoonimehr, N. (2013), "Entropy generation in steady MHD flow due to a rotating porous disk in a nanofluid", *International Journal of Heat and Mass Transfer*, Vol. 62, pp. 515-525.

Reddy, M.G., Sudha Rani, M.V.V.N.L., Ganesh Kumar, K. and Prasannakumara, B.C. (2018), "Cattaneo–Christov heat flux and non-uniform heat-source/sink impacts on radiative Oldroyd-B two-phase flow across a cone/wedge", *Journal of the Brazilian Society of Mechanical Sciences and Engineering*, Vol. 40 No. 2, pp. 1-21.

Rohni, A.M. (2012), "Flow over an unsteady shrinking sheet with suction in a nanofluid", *International Conference Mathematical and Computational Biology*, Vol. 9, pp. 511-519.

Rudraswamy, N.G., Shehzad, S.A., Ganesh Kumar, G. and Gireesha, B.J. (2017), "Numerical analysis of MHD three-dimensional Carreau nanoliquid flow over bidirectionally moving surface", *Journal of the Brazilian Society of Mechanical Sciences and Engineering*, Vol. 39 No. 12, pp. 5037-5047.

Sharidan, S., Mahmood, T. and Pop, I. (2006), "Similarity solutions for the unsteady boundary layer flow and heat transfer due to a stretching sheet", *International Journal of Applied Mechanics and Engineering*, Vol. 11, pp. 647-654.

Srinivas, R.C., Naikoti, K. and Rashidi, M.M. (2017), "MHD flow and heat transfer characteristics of Williamson nanofluid over a stretching sheet with variable thickness and variable thermal conductivity", *Transactions of A. Razmadze Mathematical Institute*, Vol. 171 No. 2, pp. 195-211.

Yao, S., Fang, T. and Zhong, Y. (2011), "Heat transfer of a generalized stretching/shrinking wall problem with convective boundary conditions", *Communications in Nonlinear Science and Numerical Simulation*, Vol. 16 No. 2, pp. 752-760.

Further reading

Williamson, R.V. (1929), "The flow of pseudoplastic materials", *Industrial & Engineering Chemistry Research*, Vol. 21 No. 11, pp. 1108-1111.

Corresponding author

Aurang Zaib can be contacted at: zaib20042002@yahoo.com